Hyperconjugative Effects in Carbenium and Silicenium Ions

Harold Basch,* Tova Hoz, and Shmaryahu Hoz

Department of Chemistry, Bar Ilan University, Ramat Gan 52900, Israel

Received: March 30, 1999; In Final Form: June 5, 1999

Bond dissociation energy (R_3M^+-L) and bond length (R−M and M−L) trends in the R_3ML^+ series of cation−ligand (L) complexes for M = carbon and silicon, and R = H, CH_3 and F are derived from density functional theory calculations using the hybrid B3LYP exchange−correlation potential. The ligands studied are NH_3, H_2O, HCN, H_2CO, MeCN, Me_2O, Me_2CO, FCN, F_2O, F_2CO, and NF_3, where ligand binding to M is through the nitrogen or oxygen atom. For all ligand substrates, R_3M^+-L bond energies are calculated to decrease from carbenium to silicenium with R = H but to increase for R=methyl and fluorine. Also for these latter two cases, in going from the bare R_3M^+ cation to the ligand complexes, the R−M distances increase by more than twice as much for the carbenium than for the silicenium ions. These trends indicate the relative importance of a stabilizing R−M hyperconjugative interaction in the bare *tert*-butyl and trifluoromethyl cations compared with the other bare cations and all the cation−ligand complexes. Ab initio, multiconfiguration VBSCF calculations are carried out on model systems ($AH_n-MH_2^+$; M = C, Si; $AH_n = CH_3$, SiH_3, F), designed to mimic the R_3M^+ cations, in order to analyze the electronic structure of the R−M bond. The π bond component, representing the hyperconjugative interaction, is found to preferentially stabilize $CH_3CH_2^+$ over $SiH_3CH_2^+$, and FCH_2^+ relative to $FSiH_2^+$. The fluorosilicenium cation shows significant π donor effects. This analysis establishes the theoretical basis for the trends in energy and structural properties found for the R_3M^+ cations and cation−ligand complexes.

1. Introduction

There are a number of interesting trends in comparing bonding properties between first and second row atom compounds.[1] For example, in going from R_3C-X to R_3Si-X, homolytic bond dissociation energies (BDE) sometimes increase and sometimes decrease, depending on the nature of the X substituent.[2−8] The more electronegative bonding species, such as X binding through O, N, or a halogen, have larger silyl−X bond energies compared to R_3C-X. The reverse is true for X groups that bond through C, S, and P atoms, for example, including X = H, where the R_3C-X BDE are larger. The impression obtained from this division is that $R_3Si^\bullet$ bonds better ionically while $R_3C^\bullet$ forms a better covalent bond. The greater tendency to ionic character of R_3Si-X bonds seems to be inconsistent with the general inability to identify bare R_3Si^+ cations in solution free of significant anion or solvent interaction. The search for free R_3Si^+ in condensed phase has been the subject of intense interest and study and has generated no little controversy.[9−16] The consensus opinion seems to be that R_3Si^+ has a high affinity for binding even the weakest nucleophilic solvent or ligand molecules due to the concentration of positive charge on the silicon atom.[3,14−18] Therefore, the bare R_3Si^+ species will be attainable only under special circumstances, such as when the approach to the Si^+ site is effectively blocked sterically, either from the R_3Si^+ side or the ligand side, or when the charge on the silicenium ion is dispersed over several atoms.[17]

Much of the interest in silyl cations derives from an analogy to the well characterized carbenium ions.[19] While the relative behaviors of R_3C^+ and R_3Si^+ with different coordinating groups have been explored,[3,12,13,20−22] less attention has been paid to relative substituent effects such as the nature of the R group.[3,23,24] Different R groups can stabilize cation centers to different degrees and the effect can be different for silicon and carbon cations. In particular, the hyperconjugative effect of the R = methyl (Me) substituent on R_3Si^+-L and R_3C^+-L stabilities, compared to R = H, has been noted(3) but not well documented quantitatively in a direct manner. What is lacking here are experimentally determined cation ligand binding energies for a wide range of R and L groups or the analogous data from high level ab initio calculations.

Recent advances in the development of theoretical methods has brought density functional theory (DFT) to the forefront.[25−27] In particular, these advances have included the use of gradient corrected exchange and correlation potentials and the addition of an exact Hartree−Fock (HF) exchange component.[28−30] These new hybrid functionals have been shown to be useful and accurate tools for computing geometric structures, vibrational frequencies, and bond dissociation energies.[25,27,29−33] The most often quoted level of accuracy comparable to DFT for closed shell systems is the MP2 level of perturbation theory.[26] R_3ML^+ complexes, where M is carbon or silicon and L is a closed shell ligand or solvent molecule, should be eminently suited for treatment by hybrid DFT and should give accurate geometries and cation−ligand bond dissociation energy values. This approach has been taken here to generate optimized geometries and cation−ligand BDE for a representative choice of R, M, and L species. The results are analyzed in terms of trends in the calculated geometric parameters and BDE as a function of the constituent components of the R_3M^+-L complex. We focus particularly on the R−M bond and on the electronic structure factors of this bond that affect these trends, such as hyperconjugation, delocalization, and resonance. These latter interrelated terms are all accommodated within valence bond (VB) language and ab initio VB theory can be brought to bear in defining the

10.1021/jp991083c CCC: $18.00
Published on Web 07/28/1999

TABLE 1: Geometry Optimized DFT(B3LYP) Energies (in au) for R_3ML^+ Using the 6-311G(2d,p) Basis Set[a]

	DFT(B3LYP) Energy						
L	ligand	H_3CL^+	H_3SiL^+	Me_3CL^+	Me_3SiL^+	F_3CL^+	F_3SiL^+
b		−39.492 093	−290.963 649	−157.600 441	−409.051 148	−337.336 493	−588.943 689
NH_3	−56.577 443	−96.250 042	−347.668 015	−214.247 555	−465.715 786	−394.036 844	−645.676 791
OH_2	−76.448 839	−116.063 033	−367.508 861	−234.077 047	−485.563 552	−413.854 526	−665.514 673
NCH	−93.453 857	−133.087 833	−384.515 892	−251.085 353	−502.566 175	−430.857 148	−682.518 484
OMe_2	−155.075 988	−194.715 714	−446.152 890	−312.709 908	−564.197 719	−492.514 638	−744.167 858
OCH_2	−114.539 321	−154.159 605	−405.598 911	−272.167 595	−523.650 805	−451.951 684	−703.605 808
NCMe	−132.795 992	−172.452 121	−423.880 706	−290.446 008	−541.926 713	−470.228 065	−721.889 026
$OCMe_2$	−193.217 780	−232.866 301	−484.304 671	−350.859 461	−602.348 339	−530.665 001	−782.320 927
NCF	−192.695 147	−232.320 684	−483.753 423	−350.318 944	−601.803 724	−530.093 230	−781.757 059
OF_2	−274.747 730	−314.293 957	−565.738 169	−432.352 532	−683.808 782	−612.092 946	−863.727 077
OCF_2	−313.115 305	−352.701 134	−604.148 889	−470.782 402	−722.203 941	−650.491 551	−902.153 415
NF_3	−354.191 231	−393.782 108	−645.201 723	−511.795 580	−763.264 776	−691.553 482	−943.194 333

[a] Connectivity is to the left-most atom in L. [b] Bare R_3M^+ cation.

contributing bonding configurations and the importance of each type in such an analysis.

In this regard, quantitative VB theory has recently been applied to the interpretation and understanding of a wide variety of electronic structure effects.[18,34−40] In particular, to study the special interactions in the R−M bond of carbenium and silicenium cations simple AH_n−MH_2^+ model systems (AH_n = CH_3, SiH_3, F) are used here to represent the interaction of saturated methyl, silyl and fluorine substituents (R) with cation centers (M^+) in the parent R_3M^+ ions. These model systems are VB analyzed for the various bonding component interactions that determine the total electronic and geometric structure description. Besides the usual electron pair σ bond between M^+ and A, with its covalent and ionic components,[2,41] the possibility of an additional, π type bond between the saturated AH_n group and the electron deficient MH_2^+ fragment is the key to the presence and magnitude of the hyperconjugative effect.[42] In this context the hyperconjugative interaction can also be termed a resonance effect between σ bond and $\sigma + \pi$ bond VB configurations, or a delocalization from an electron rich AH_n to an electron deficient MH_2^+. The added π interaction can affect geometric structure parameters and the M−L bond energies by being operative in both the parent cation and the R_3M^+−L complexes to different degrees. Therefore, we bring here a combination of DFT determined geometry and energy values for a wide range of R_3M^+−L complexes and a VB analysis showing how σ, π bonding interactions in the R−M^+ bond can affect these values.

2. Methods and Results

The geometric structures of all the R_3M^+−L complexes with R = H, CH_3, and F; M = C and Si; and L = NH_3, H_2O, HCN, H_2CO, MeCN, Me_2O, Me_2CO, FCN, F_2O, F_2CO, and NF_3 were gradient optimized using the hybrid B3LYP exchange−correlation potential in the DFT method.[43,44] All coordination of L to M in the complexes is through the nitrogen or oxygen atom of the ligand. The optimized geometries of the bare R_3M^+ and neutral ligands were also generated. In all cases, the standard 6-311G(2d,p) basis set was used with five d components.[44] In the case of the bare cations the nature of the optimized geometry at the equilibrium structure was established by a harmonic force field frequency calculation using analytical second derivatives. Analogous frequency calculations were not carried out on the associated complexes because of their high computer time demands. This could affect mainly the Me_3C^+ and Me_3Si^+ complexes where a given optimized geometry may not be the global minimum with respect to the relative orientations of the methyl groups. Different conformers can be generated by rotations about the C−C or C−Si bonds. An analogous uncertainty involves the Me_2O and Me_2CO ligand complexes for the same reason. The energy difference between the various low energy rotamer conformations of the methyl groups is expected to be in the range of, at most, several tenths of a kcal/mol. The major geometric parameters discussed here, the C−C, C−Si, F−C, F−Si, C−N, Si−N, C−O, and Si−O bond lengths, are not expected to be significantly affected by rotational isomerism of the methyl groups.

TABLE 2: R_3M^+−L Binding Energies[a]

	binding energy (kcal/mol)					
L	H_3C^+	H_3Si^+	Me_3C^+	Me_3Si^+	F_3C^+	F_3Si^+
NH_3	113.3	79.6	43.7	54.4	77.1	97.7
OH_2	76.6	60.5	17.4	39.6	43.4	76.6
NCH	89.0	61.7	19.5	38.1	41.9	75.9
OMe_2	92.6	71.1	21.0	44.0	64.1	93.0
OCH_2	80.4	60.2	17.5	37.6	47.6	77.1
NCMe	102.9	76.0	31.1	49.6	60.0	93.7
$OCMe_2$	98.2	77.3	25.9	49.5	69.5	100.1
NCF	83.7	59.4	14.7	35.7	38.6	74.2
OF_2	35.9	18.7	(4.2)[b]	7.8	7.4	24.3
OCF_2	58.8	43.9	7.9	23.2	24.9	59.2
NF_3	62.0	29.4	2.5	13.8	16.2	37.3

[a] Connectivity is to the left-most atom in L; from DFT(B3LYP)/6-311G(2d,p) energies in Table 1. [b] Binding through F.

TABLE 3: R_3M^+−L Bond Lengths[a]

	M−L Bond Lengths					
Y	H_3C^+	H_3Si^+	Me_3C^+	Me_3Si^+	F_3C^+	F_3Si^+
NH_3	1.514	1.914	1.558	1.947	1.536	1.854
OH_2	1.522	1.849	1.707	1.914	1.589	1.774
NCH	1.436	1.874	1.492	1.929	1.554	1.830
OMe_2	1.483	1.799	1.646	1.863	1.489	1.724
OCH_2	1.489	1.830	1.670	1.889	1.566	1.765
NCMe	1.436	1.841	1.487	1.888	1.500	1.792
$OCMe_2$	1.473	1.780	1.599	1.833	1.475	1.710
NCF	1.448	1.872	1.525	1.933	1.558	1.821
OF_2	1.549	2.064	(4.020)	2.297	2.252	1.988
OCF_2	1.517	1.857	2.873	1.965	1.625	1.771
NF_3	1.498	2.032	3.110	2.146	1.752	1.982

[a] Connectivity is to the left-most atom in Y. Distances in angstroms; from DFT(B3LYP)/6-311G(2d,p) optimized geometries.

The results of the DFT(B3LYP)/6-311G(2d,p) calculations are presented in Tables 1−5. Table 1 tabulates the total electronic energies of the bare cation and complex species. Table 2 tabulates the R_3M^+−L BDE values, taken directly from the data in Table 1 with no correction for zero point vibrational energy (ZPE) differences or basis set superposition error (BSSE).[45] DFT is known to suffer less from BSSE than other post-Hartree−Fock (HF) methods such as MP2 or incomplete CI. Table 3 shows the optimized M−L bond lengths. The corresponding optimized R−M distances are listed in Table 4. Mulliken atomic charges for the atoms involved in the M−L bond are shown in Table 5. Selected structures are shown in

TABLE 4: R−M Bond Lengths in R_3M^+L Complexes[a]

	R−M bond lengths (Å)[b]			
L	Me_3C^+ C−C	Me_3Si^+ C−Si	F_3C^+ F−C	F_3Si^+ F−Si
c	1.459	1.833	1.236	1.525
NH_3	1.526	1.855	1.309	1.551
OH_2	1.504	1.848	1.287	1.545
NCH	1.434	1.853	1.296	1.546
OMe_2	1.513	1.855	1.305	1.553
OCH_2	1.507	1.851	1.292	1.547
NCMe	1.533	1.855	1.305	1.550
$OCMe_2$	1.516	1.855	1.307	1.554
NCF	1.529	1.852	1.295	1.546
OF_2	1.458	1.839	1.245	1.536
OCF_2	1.459	1.847	1.283	1.545
NF_3	1.460	1.844	1.279	1.540

[a] Connectivity is to the left-most atom in Y; data from DFT(B3LYP)/6-311G(2d,p) optimized geometries. [b] Averaged over the three same-type bonds. [c] Bare R_3M^+ cation.

Figure 1. Structures **1** and **2** display the equilibrium conformations for the bare Me_3C^+ and Me_3Si^+ cations, respectively. Structures **3**−**14** show representative example geometries of the cation complexes for each ligand.

VBSCF calculations using the TURTLE[46−48] computer program were carried out on the $CH_3-CH_2^+$, $CH_3-SiH_2^+$, $SiH_3-CH_2^+$, $F-CH_2^+$, and $F-SiH_2^+$ model systems, denoted generically here as $AH_n-MH_2^+$, with $n = 3$ for the first three ions and $n = 0$ for the last two. The geometries were obtained by ab initio gradient optimization, where the C−H and Si−H bonds within a given group (CH_3, SiH_3, CH_2, SiH_2) were constrained to be equivalent. These limitations were adopted so that the model system geometries would have the classical ethyl form and not the nonclassical bridged or near-bridged structures.[3] Unconstrained geometry optimization of $CH_3CH_2^+$ produces the symmetrically protonated ethylene geometry.[49,50] $SiH_3CH_2^+$ rearranges with no barrier to $CH_3SiH_2^+$, which has a near-classical structure. Unconstrained geometry optimization introduces a small amount of asymmetry about the carbon and silicon atoms in $CH_3SiH_2^+$ and $FSiH_2^+$. FCH_2^+ is unaffected by the C−H equivalency constraints. The VB calculations were carried out using the constrained, equivalent bond geometries.

The atomic basis sets used to produce all the model system geometries consist of the Dunning[51] double-ζ [4s2p] contraction of Huzinaga's (9s5p) optimized Gaussians[52] for carbon, the 6-311G double-ζ set for Si, and the [311] contracted set for the hydrogen atom from the Gaussian94 program.[44] In addition, single Gaussian d-type polarization functions (five components) were added to the carbon (exponent = 0.7500), silicon (exponent = 0.4500), and fluorine (exponent = 0.9000) atoms. This basis set will be denoted DZP.

The $AH_n-MH_2^+$ model system geometries were generated at the CAS(4,4)/MCSCF theory level[53] with the DZP basis set. CAS(4,4) distributes 4 electrons among four molecular orbitals using all possible configurations consistent with a spin singlet ($S = 0$) state and the spatial symmetry of the electronic ground state. Using the HF electronic configuration as a reference, the two orbitals being correlated here hold the A−M σ bonding pair of electrons and the combination of A−H bonding orbitals that have the same symmetry as the empty M orbital in MH_2^+. The resultant constrained optimized bond lengths and angles are shown in Table 6. The geometries for $CH_3CH_2^+$, $CH_3SiH_2^+$ and $SiH_3CH_2^+$ have the MH_2^+ plane aligned perpendicular to one of the A−H bonds with close to C_s symmetry.

The VB analysis focuses on the A−M bond in the $AH_m-MH_2^+$ systems. AH_m (CH_3, SiH_3, F) and MH_2^+ (CH_2^+, SiH_2^+) are taken as the interacting fragments, where all the VB orbitals are localized either on the AH_n or MH_2^+ groups. These two fragments will be generally labeled a and m, respectively, for the purpose of identifying the fragment parentage of the VB orbitals and the fragment charges. All the orbitals of a given fragment are expanded in the combined atom centered basis functions of that fragment only. The orbitals in each fragment group are divided into an active and a passive set, where the passive set orbitals are doubly occupied in all the VB configurations. Each of the variably occupied orbitals can have occupancies of 0, 1, or 2, depending on the configuration. The active set consists of the σ_a and σ_m fragment orbitals that form the A−M σ bond, and the π_a and π_m orbitals that can form the hyperconjugative interaction. π_m is the empty MH_2^+ fragment orbital and π_a is the corresponding symmetry combination of A−H bond orbitals that is doubly occupied in AH_n. These descriptions are actually anticipatory since the exact forms of all the active and passive orbitals are determined by the VBSCF procedure.

In terms of the active π_a, σ_a, σ_m, and π_m VB orbitals, the classical description of the singlet spin-paired $AH_n-MH_2^+$ σ bond is described by configurations (1) to (3):[2]

$$(a^0m^+) \qquad \pi_a^{\,2}\sigma_a^{\,1}\sigma_m^{\,1}\pi_m^{\,0} \tag{1}$$

$$(a^+m^0) \qquad \pi_a^{\,2}\sigma_a^{\,0}\sigma_m^{\,2}\pi_m^{\,0} \tag{2}$$

$$(a^-m^{2+}) \qquad \pi_a^{\,2}\sigma_a^{\,2}\sigma_m^{\,0}\pi_m^{\,0} \tag{3}$$

where in all the VB configurations described here the doubly occupied passive orbitals are not listed explicitly. The formal charge distribution between fragments is indicated in parentheses to the left of each configuration.

To describe the hyperconjugative effect, which is a charge transfer or delocalization from AH_n to MH_2^+, configuration (4) must be added:

$$(a^+m^0) \qquad \pi_a^{\,1}\sigma_a^{\,1}\sigma_m^{\,1}\pi_m^{\,1} \tag{4}$$

This configuration represents simultaneous spin-coupled σ and π bonds between the a and m fragments. The four open shell system can be coupled to give an overall singlet spin state in two ways, representing the coupling between spin-singlet each and spin-triplet each a^+ and m^0 fragments. Therefore, configuration (4) gives rise to two linearly independent VB structures whose weights are determined separately in the VBSCF variational calculations to be described. Additional configurations can be constructed distributing the 4 electrons among the four active orbitals. If these are limited to electron distributions that always have two σ and two π electrons then the following configurations can be added:

$$(a^0m^+) \qquad \pi_a^{\,1}\sigma_a^{\,2}\sigma_m^{\,0}\pi_m^{\,1} \tag{5}$$

$$(a^+m^0) \qquad \pi_a^{\,0}\sigma_a^{\,2}\sigma_m^{\,0}\pi_m^{\,2} \tag{6}$$

$$(a^{2+}m^-) \qquad \pi_a^{\,1}\sigma_a^{\,0}\sigma_m^{\,2}\pi_m^{\,1} \tag{7}$$

$$(a^{2+}m^-) \qquad \pi_a^{\,0}\sigma_a^{\,1}\sigma_m^{\,1}\pi_m^{\,2} \tag{8}$$

Configurations 5 and 7 each have a covalent π bond and no σ bonds. Configuration (6) has no bonds at all and configuration (8) has only a σ bond. Only (5) has the same a^0m^+ fragment charge distribution as the parent configuration (1). In a multi-

TABLE 5: Mulliken Atomic Charges[a]

	H_3CL^+			H_3SiL^+			Me_3CL^+			Me_3SiL^+			F_3CL^+			F_3SiL^+		
L	H[b]	C	L	H[b]	Si	L	C[b,c]	C	L	C[b,c]	Si	L	F[b]	C	L	F[b]	Si	L
d	0.259	0.224		0.078	0.766		0.245	0.119		−0.519	1.056		0.003	0.990		−0.389	2.146	
NH_3	0.176	−0.156	−0.277	0.0	0.649	−0.539	−0.204	−0.130	−0.292	−0.537	1.072	−0.523	−0.198	0.964	−0.315	−0.473	2.017	−0.523
OH_2	0.187	−0.030	−0.273	0.003	0.752	−0.504	−0.201	−0.019	−0.335	−0.536	1.104	−0.473	−0.150	1.003	−0.306	−0.461	2.119	−0.505
NCH	0.195	−0.098	−0.062	0.007	0.714	−0.315	−0.200	−0.036	−0.111	−0.525	1.098	−0.271	−0.163	1.030	−0.188	−0.467	2.046	−0.276
OMe_2	0.164	−0.032	−0.379	−0.019	0.771	−0.653	−0.224	0.067	−0.448	−0.559	1.212	−0.617	−0.205	1.075	−0.420	−0.478	2.129	−0.701
OCH_2	0.174	−0.024	−0.160	−0.004	0.748	−0.392	−0.223	0.041	−0.223	−0.540	1.126	−0.354	−0.166	1.006	−0.206	−0.468	2.098	−0.404
NCMe	0.181	−0.101	−0.122	−0.009	0.723	−0.400	−0.204	−0.007	−0.180	−0.526	1.106	−0.350	−0.184	1.010	−0.221	−0.479	2.039	−0.361
$OCMe_2$	0.159	−0.054	−0.264	−0.024	0.745	−0.529	−0.217	0.062	−0.320	−0.541	1.154	−0.493	−0.205	1.014	−0.298	−0.483	2.084	−0.553
NCF	0.192	−0.087	−0.097	0.005	0.724	−0.340	−0.199	−0.027	−0.161	−0.526	1.107	−0.293	−0.163	1.037	−0.222	−0.469	2.055	−0.298
OF_2[e]	0.220	0.012	0.225	0.049	0.683	0.122	−0.244	0.114	0.238	−0.534	1.083	0.141	−0.044	1.001	0.159	−0.428	2.075	0.114
OCF_2	0.182	−0.034	−0.202	0.007	0.728	−0.411	−0.237	0.122	−0.371	−0.537	1.095	−0.361	−0.149	1.009	−0.268	0.463	2.091	−0.425
NF_3	0.206	−0.082	−0.716	0.037	0.654	0.559	−0.237	0.093	0.554	−0.535	1.029	0.580	−0.134	0.992	0.677	−0.446	2.036	0.576

[a] Charge for the L group is for the coordinating (nitrogen or oxygen) atom alone; data from DFT(B3LYP)/6-311G(2d,p) optimized geometries. [b] Averaged over the three atoms. [c] Methyl group carbon atom. [d] Bare cation. [e] Binding through F.

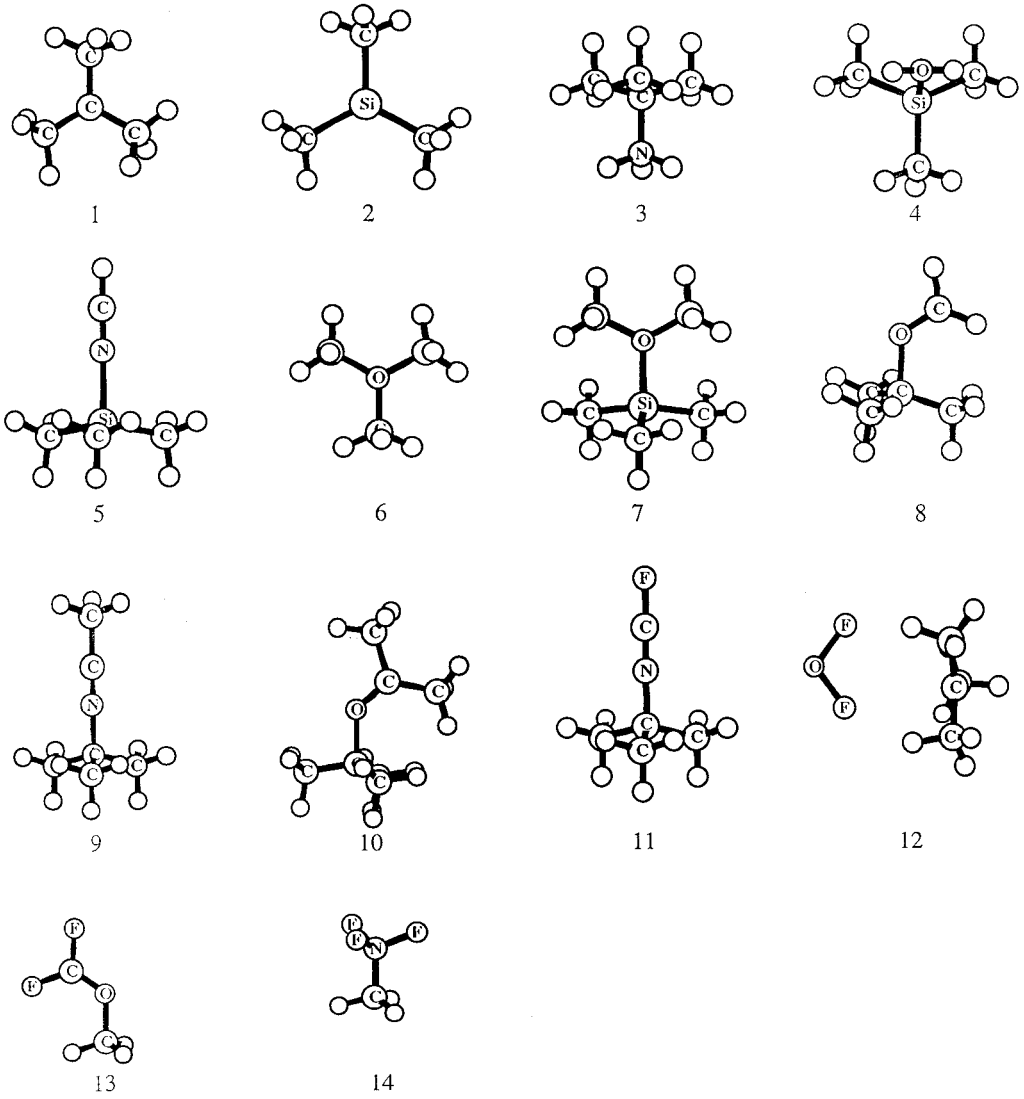

Figure 1. 1, Me_3C^+; **2**, Me_3Si^+; **3**, $Me_3CNH_3^+$; **4**, $Me_3SiOH_2^+$; **5**, Me_3SiNCH^+; **6**, $H_3COMe^+{}_2$; **7**, $Me_3SiOMe_2^+$; **8**, $Me_3COCH_2^+$; **9**, $Me_3SiNCMe_2^+$; **10**, $Me_3COCMe_2^+$; **11**, Me_3CNCF^+; **12**, $Me_3COF_2^+$; **13**, $H_3COCF_2^+$; **14**, $H_3CNF_2^+$.

configuration VB expansion, the weights of configurations (4) to (8) give the relative importance of occupying the π_m orbital, and hence the magnitude of the hyperconjugative effect. The total VB wave function is a linear combination of some or all of the configurations (1) to (8). All the active and passive VB orbitals and the structure expansion coefficients are determined by the VBSCF procedure.[46−48,54] Both the AH_n (CH_3 and F) and MH_2^+ (CH_2^+) fragment orbitals were expanded in the same DZP basis set[44,51,52] described above for the CAS(4,4) geometry optimizations of the model cation systems. For reasons of economy, the VBSCF calculations on $CH_3SiH_2^+$ and $SiH_3CH_2^+$ were carried out using compact effective potentials (CEP) and valence electron basis sets[55,56] instead of the all electron set. The shared exponent CEP basis sets are valence double-ζ. The DZP set of d-type polarization basis functions for carbon, silicon, and fluorine and the 311 split set for the hydrogen atom described above were also used with the CEP basis sets. This basis set will be called VDZP. The use of the effective potential

TABLE 6: Equilibrium Geometries of Model $AH_nMH_2^+$ Systems[a]

	bond length (Å)			angles (deg)		
$AH_mMH_2^+$	A−M	A−H[b]	M−H[c]	HAM[b]	HMA[c]	HMH
$CH_3CH_2^+$	1.455	1.087	1.077	109.8	121.5	116.9
$CH_3SiH_2^+$	1.857	1.091	1.457	110.4	121.7	116.6
$SiH_3CH_2^+$	1.976	1.463	1.081	102.2	123.4	113.2
FCH_2^+	1.243		1.078		116.9	126.1
$FSiH_2^+$	1.550		1.448		116.2	127.5

[a] CAS(4,4)/DZP optimized geometries with equivalency constraints among the AH_n and MH_2^+ groups. [b] All A−H bonds have equivalent A−H lengths and HAM angles. [c] All M−H bonds have equivalent M−H lengths and HMA angles.

TABLE 7: Binding Energies as a Function of VB Configuration List[a]

$AH_nBH_2^+$[g]	$CH_3CH_2^+$[b]	$CH_3SiH_2^+$	$SiH_3CH_2^+$	FCH_2^+[b]	$FSiH_2^+$[b]
RHF[e]	117.8	83.7[b]	102.2[b]	103.2	107.2
GVB[e]	126.2	91.7[b]	110.1[b]	115.5	110.7
CAS(4,4)[e]	135.6	103.8[b]	116.7[b]	144.3	139.2
VBSCF[d]					
I	88.5	64.9[c]	59.6[c]	14.6	6.2
II	104.2	72.6[c]	103.1[c]	21.7	8.0
III	107.6	82.3[c]	103.2[c]	76.1	91.4
IV	124.9	80.8[c]	106.5[c]	104.7	64.9
V	126.8	88.2[c]	106.9[c]	124.4	114.8
VI	132.3	95.8[c]	110.3[c]	137.3	134.0
DFT(B3LYP)[f]	149.5	102.9[b]	132.0[b]	151.5	139.6
G2	*h*	104.9	*i*	152.4	148.4

[a] Electronic energy differences between $AH_nMH_2^+$ and $AH_n + MH_2^+$. The latter are single-configuration radical states; VBSCF values are interpolated energy minima from a one-dimensional grid. [b] All electron calculation. [c] VDZP/CEP calculation. [d] CAS(4,4) optimized geometry. Theory levels I−VI are described in the text. [e] DZP basis optimized geometry. [f] 6-311+G(2d,p) basis set optimized geometry. [g] Equivalent C−H and Si−H bonds within each AH_n or MH_2^+ group, except for G2 calculation. [h] Forms nonclassical bridge structure. [i] Converts spontaneously to $CH_3SiH_2^+$.

to replace the chemically inert core electrons (1s on C and 1s to 2p on Si) substantially reduces the number of VB orbitals and leads to a significant reduction in computer resources needed for the VBSCF calculations.

Separate VBSCF calculations were carried out using six different combinations (I−VI) of configurations (1) to (8) for each of the five model cation systems. VBSCF(I) optimizes the single configuration (1) alone. This is the simplest VB representation of a chemical bond: the Lewis structure. VBSCF(II) adds configuration (2) to set I. The a^+m^0 charge transfer state is ordinarily expected to be the major interacting configuration with (1) for a description of the A−M σ bond. VBSCF(III) includes configurations (1) to (3) and, compared to VBSCF-(II), gives the relative importance of the reverse charge transfer a^-m^{2+} distribution to the A−M σ bond. VBSCF(III) represents the classical three configuration description of the chemical bond in terms of localized fragment orbitals. VBSCF(IV) adds configurations (4) to (6) to VBSCF(II). Compared to the set II results, VBSCF(IV) will show the importance of the $\pi_a-\pi_m$ hyperconjugative interaction. VBSCF(V) adds configurations (3), (7), and (8) to set IV and completes the full expansion of all eight configurations in one VBSCF calculation. All resonance interactions between the localized fragment configurations are included at this level.

VBSCF(VI) abandons the localized fragment description of the $AH_nMH_2^+$ systems and allows unrestricted delocalized mixing among the fragments. VBSCF of configuration (1) alone with interfragment delocalization mixing among all the orbitals is equivalent to a single electron pair GVB[55,57,58] or CAS-(2,2)[53] calculation. Such mixing effectively introduces ionic terms directly into the configurations with the original a^0m^+ charge distribution configurations (1) and (5). Therefore, VB-SCF(VI) is a two configuration expansion consisting of configurations (1) and (5), with unrestricted delocalized mixing among the fragment orbitals. VBSCF(V) and VBSCF(VI) should be close to the full reference CAS(4,4) description of the $AH_n-MH_2^+$ model systems.

TABLE 8: Heavy Atom Bond Lengths as a Function of VB Configuration List

	A−M(A)[a]				
$AH_nMH_2^+$[g]	$CH_3CH_2^+$[b]	$CH_3SiH_2^+$[c]	$SiH_3CH_2^+$[c]	FCH_2^+[b]	$FSiH_2^+$[b]
VBSCF[d]					
I	1.486	1.884	1.917	1.444	2.018
II	1.468	1.907	2.005	1.489	2.025
III	1.467	1.890	2.003	1.345	1.588
IV	1.460	1.882	1.984	1.254	1.495
V	1.466	1.875	1.980	1.260	1.554
VI	1.458	1.865	1.983	1.241	1.547
CAS(4,4)[b,d]	1.455	1.857	1.976	1.243	1.550
DFT(B3LYP)[b,f]	1.411	1.818	1.902	1.232	1.547

[a] A−B bond lengths in $AH_nMH_2^+$; VBSCF values are interpolated equilibrium bond lengths from one-dimensional grid. [b] All electron calculation. [c] VDZP/CEP calculation. [d] DZP basis; CAS(4,4) optimized geometry for the AH_n and MH_2^+ fragments. Configuration compostion at each level (I, II, ...) is described in the text. [e] DZP basis optimized geometry. [f] 6-311+G(2d,p) basis set optimized geometry. [g] Equivalent C−H and Si−H bonds within each AH_n or MH_2^+ group.

VBSCF ground-state wave functions and energies for all the $AH_n-MH_2^+$ were generated pointwise by stepping through the A−M distance around the energy minimum for each of the configuration sets (I to VI). The local AH_3 and MH_2^+ geometries were frozen at their CAS(4,4) optimized values. The equilibrium A−M distance and binding energy relative to $AH_n + MH_2^+$ was then derived by quadratic interpolation from the surrounding points. The calculated binding energies are tabulated in Table 7 and the bond lengths in Table 8. All the binding energies are referenced to the same $AH_3 + MH_2^+$ asymptotes, to which all the I to VI configuration sets dissociate.

Because of the nonorthogonality of the VB orbitals the nine singlet spin coupled structures constructed from configurations (1) to (8) are also nonorthogonal. The weight (W_i) of each structure i is calculated from,[59]

$$W_i = C_i \sum_j C_j S_{ij} \tag{9}$$

where S_{ij} is the overlap integral between structures and the $\{C_i\}$ are the structure expansion coefficients in each VBSCF calculation. The sum over j runs over the number of structures in the particular set expansion I to VI. The calculated weights for VBSCF(V) for all the $AH_n-MH_2^+$ model systems at their respective CAS(4,4) optimized geometries are shown in Table 9. Like the Mulliken population analysis in molecular orbital theory, structure weights W_i can also take on negative values which are difficult to interpret.

3. Discussion

The order of the discussion is as follows. The optimized R_3M^+ cations and R_3ML^+ complexes will be presented; after which the trends in their calculated properties will be explored. The VB analysis of the model $AH_nMH_2^+$ systems will then be discussed and connected to the R_3ML^+ results.

A detailed computational investigation of the structures and energies of the various possible $C_4H_9^+$ isomers has recently been reported using ab initio post-HF theory level methods, with a

TABLE 9: Weights of VB Configurations[a]

$AH_nMH_2^+$ [d,e] = VB configuration	$CH_3CH_2^+$ [b]	$CH_3SiH_2^+$ [c]	$SiH_3CH_2^+$ [c]	FCH_2^+ [b]	$FSiH_2^+$ [b]
(1)	0.553	0.623	0.519	0.417	0.421
(2)	0.226	0.176	0.409	0.061	0.001
(3)	0.055	0.131	0.010	0.157	0.386
(4)[g]	−0.004	−0.003	−0.001	-0.014	−0.008
	0.126	0.049	0.045	0.180	0.043
(5)	0.038	0.026	0.008	0.201	0.166
(6)	−0.001	0.000	0.000	0.006	0.000
(7)	0.006	0.002	0.010	−0.005	−0.007
(8)	0.000	−0.001	0.000	−0.003	−0.002

[a] According to eq 9. Weights are for VBSCF(V). [b] All electron calculation. [c] VDZP/CEP calculation. [d] DZP basis; CAS(4,4) optimized geometry. [e] Equivalent C−H and Si−H bonds within each AH_n or MH_2^+ group. [f] Same configuration numbering as in text. [g] Two VB structures.

comprehensive review of previous calculational treatments.[60] For the *tert*-butyl cation (Me_3C^+) of interest here, three energetically close-lying geometric structures have been identified, having symmetries C_s, C_{3h}, and C_{3v}. The MP4(SDTQ) energy difference between the C_s and C_{3h} structures was found to be only 0.1 kcal/mol, and the C_{3v} conformer was ∼1 kcal/mol higher.[60] The unconstrained DFT(B3LYP)/6-311G(2d,p) optimized geometry obtained here gives the D_{3h}-type structure shown in **1**, with one hydrogen atom (H′) on each methyl group approximately coplanar with the frame of the four carbon atoms. The actual deviation of the dihedral H′CCC angles from planarity is in the 7°−8° range. The calculated C−C distances are very close and average to 1.459 Å, which agrees very well with the experimental estimate of 1.46−1.47 Å[61] and the previously calculated value of 1.46 Å.[60] The harmonic frequency calculation shows all real frequencies for this structure. The expected distortions from the ideal methyl group geometry of equivalent bond lengths and angles due to hyperconjugative interactions between the perpendicular C−H bonds and the corresponding "vacant" p orbital on the central carbon atom, are also observed.[60,62] Because of the dihedral H′CCC tilt and corresponding alignment of the other C−H bonds on each methyl group, there are three different C−H bond lengths on each methyl group, instead of the two different distances expected from perfect D_{3h} symmetry. These distances are 1.087, 1.096, and 1.104 Å, with the smallest value belonging to the near-in-plane C−H′ bonds. The corresponding HCC angles are calculated to be 106°, 111°, and 114.5°, with the latter belonging to the H′CC angles.

The trimethyl silylium cation, Me_3Si^+ (**2**), has been calculated to have C_{3h} symmetry,[14,63,64] and this is also the result obtained here. The H′CSiC dihedral angles are completely planar. The difference between the methyl group H′−C and H−C bond lengths (1.097 and 1.090 Å, respectively) is only 0.007 Å. The HCSi angle is 109.5° while for H′CSi it is ∼3.5° larger at 113.0° in all three methyl groups. The Si−C bond length is a uniform 1.832 Å, compared to the best previous study at the HF level which gave 1.838 Å. Analogously, the previous study found HCSi and H′CSi angles of 109.7° and 112.6°, respectively. Thus the ab initio HF[14] and DFT results are very close. Although the different parallel and perpendicular H−C bond lengths and HCSi angles show evidence of a hyperconjugative interaction between the methyl groups and the electron deficient silicon atom, the spread in values is only about half that found for the corresponding H−C and HCC geometric parameters in Me_3C^+. This ratio is close to the estimated ratio of stabilization by complete methyl substitution of H_3C^+ and H_3Si^+ derived indirectly by isodesmic reaction cycles.[3,14,21,65]

Both Me_3C^+ and Me_3Si^+ have planar heavy atom skeletons, as expected of such cations. There is no hint of pyramidization of the cation frames, as is found in condensed phases for Me_3Si^+ even when interaction with a counterion or solvent molecule is weak.[24,66] In fact, the planarity of the C_3Si skeleton is taken as prima facie evidence of the existence of a hyperconjugative interaction between C−H and Si^+ in the perpendicular direction. Analogously, the H_3C^+, H_3Si^+, F_3C^+, and F_3Si^+ cations are calculated here to be planar. It should be noted that planarity itself gives no indication of the strength of the hyperconjugative interaction and the extent of such an interaction must be derived from other data.

As shown in Table 2, $CH_3NH_3^+ \rightarrow CH_3^+ + NH_3$ has the largest calculated binding energy of any of the cation complexes studied here. All the $R_3MNH_3^+$ complexes have a staggered conformation between the R_3M^+ and NH_3 groups across the M−N bond. The R_3M^+ cation in the complexes is pyramidalized and has C_{3v} symmetry, with a C−H bond from each methyl group aligned mutually parallel and facing away from ammonia. The geometric structure of $Me_3CNH_3^+$ is shown in **3**. The $CH_3^+-NH_3$ enthalpy of dissociation has been measured[67] at 105.2 kcal/mol compared to the calculated 113.3 kcal/mol electronic energy difference shown in Table 2. The experimental bond energies are thermodynamic enthalpies of dissociation (ΔH), whereas the DFT(B3LYP) calculated values are total energy differences (ΔE). The largest correction to ΔE to reach ΔH is the ZPE energy difference between the $R_3M^+ + L$ components and the cation complex, R_3ML^+. As a rule of thumb, the larger the binding energy and the lighter the atoms, the larger the ΔZPE correction.[7,50,66] In the case of a binding energy as large as ∼110 kcal/mol and light atoms such as CH_3^+ and NH_3, the ΔZPE correction could be as large as 8−9 kcal/mol. This size adjustment would bring the calculated and measured BDE for $CH_3^+-NH_3$ into very good agreement. However, other possible sources of errors in the energy calculations, such as the neglect of BSSE, uncertainty in the cation complex equilibrium geometry, and a possible basis set imbalance between the complex and its dissociation products, should also be considered. These latter corrections are expected to be smaller than the ΔZPE term and will tend to cancel each other, at least partially.

The reported $Me_3C^+-NH_3$ dissociation energy of 39.0 kcal/mol[67] or 46.5 kcal/mol[20,68−70] is close to the calculated ΔE value of 43.7 kcal/mol in Table 2. Given the above comments on $CH_3-NH_3^+$ the smaller binding energy value which is derived from experimental heats of formation[69] seems likely to be more accurate. The H_3Si^+ and Me_3Si^+ affinities for an ammonia molecule are (ΔE) calculated here to be 79.6 and 54.7 kcal/mol, respectively. The latter binding energy has been measured at 46.5[70] and 50[20] kcal/mol experimentally as ΔH. Olsson *et al.*[14] calculate 76.6 kcal/mol for $H_3Si^+-NH_3$ dissociation and 54.5 kcal/mol for $Me_3Si^+-NH_3$ dissociation. All these energies are in good respective agreement.

For $H_3SiNH_3^+$ and $Me_3SiNH_3^+$, the Si−N bond lengths have been calculated at the HF level to be 1.904−1.917 and 1.957 Å, respectively. The Si−C distance in the latter complex was also calculated to be 1.865 Å.[14] The corresponding DFT(B3LYP) optimized quantities in this study are 1.914, 1.947, (Table 3) and 1.833 Å (Table 4). The agreement is very good and reinforces the point of view that the binding in these type cation complexes is easily calculated.[14,71]

Almost all the $R_3MOH_2^+$ cations adopt the staggered configuration across the M−O bond, as was found for the ammonia complexes. The water complexes have a lone pair of electrons

of the oxygen atom in place of an N−H bond of ammonia, with the other oxygen atom electron pair directed at M^+ for bonding. A perspective view is shown in **4** for $Me_3SiOH_2^+$. The exception to this general conformation is the $F_3SiOH_2^+$ complex which has HOSiF dihedral angles of 6.0° and −170.5° for the two water hydrogen atoms relative to the same fluorine atom. Thus the plane of the water molecule is essentially perpendicular to the plane of fluorine atoms on opposite sides of Si^+.

The experimental methyl cation affinity of water has been (ΔH) measured at 68.5 kcal/mol[67], which is not far from the ΔE (Table 2) value of 76.6 kcal/mol. The $Me_3C^+-OH_2$ dissociation energy is (ΔH) reported at 11.0 kcal/mol[67], which is also in the range of the uncorrected 17.4 kcal/mol ΔE value in Table 2. The H_3Si^+ affinity of water is DFT(B3LYP) calculated here to be 60.5 kcal/mol and by Olsson et al.[14] to be 56−57 kcal/mol at the HF theory level. The experimental (ΔH) $Me_3Si^+-OH_2$ dissociation energy is reported at ∼31 kcal/mol[20,72,73a] and (ΔE) calculated here at 39.6 kcal/mol in Table 2. This is actually a larger difference than expected and may indicate a need to reevaluate the experimental quantity.

The Si−O distance in $H_3SiOH_2^+$ and $Me_3SiOH_2^+$ was HF calculated to be 1.859−1.846 Å and 1.910 Å, respectively.[14] The values for these geometric parameters obtained here by the DFT(B3LYP) method are 1.849 and 1.914 Å (Table 3). The Si−C distance in $Me_3SiOH_2^+$ is shown in Table 4 to be 1.848 Å, compared to the 1.860 Å HF value. Again, the HF and DFT results are in good agreement.

The geometry of the R_3MNCH^+ cation complexes is simple since the HCN ligand group is collinear with the central carbon or silicon atom in all the structures. The local Me_3C^+ and Me_3Si^+ conformations are C_{3v}, and the latter complex is shown in **5**. The DFT(B3LYP) calculated ΔE binding energies (Table 2) are (experiment in parentheses): H_3C^+-NCH 89.0 (87.1)[67,74] kcal/mol and Me_3C^+-NCH 19.5 (22.9)[67] kcal/mol. The corresponding H_3Si^+-NCH and Me_3Si^+-NCH ΔE binding energies are 61.7 and 38.1 kcal/mol, compared to HF values of 58−60 and 40.1 kcal/mol, respectively.[14] Analogously, the Si−N distances in the H_3SiNCH^+ and Me_3SiNCH^+ complexes are 1.874 Å (1.888 Å) and 1.929 Å (1.940 Å), where the numbers in parentheses are from ref 14. The Si−C distance are calculated to be 1.853 Å (1.862 Å).

The association of CH_3^+ with dimethyl ether (OMe_2) forms a symmetric pyramidal Me_3O^+ complex (**6**) with equal C−O bond lengths (1.483 Å) and COC angles (113.9°). The conformation is C_{3v} with one C−H bond on each methyl group pointing away from the oxygen atom in parallel array. Two O−C bonds and the lone pair of electrons on the oxygen atom are staggered with the C−H bonds of each methyl group. The same skeletal conformation is adopted by $H_3SiOMe_2^+$, $Me_3COMe_2^+$, $Me_3SiOMe_2^+$ (**7**), $F_3COMe_2^+$, and $F_3SiOMe_2^+$, with the respective Si−H, C−C, Si−C, C−F, and Si−F bonds in place of C−H. The relative orientation of the ether ligand methyl H−C bonds, however, is different: the H−C bond with the most planar H−C−O-M dihedral angle points generally toward Si for all the silicon cation complexes, and points away from C in all the carbenium complexes. The origin of this conformational difference between the silicenium and carbenium cations is not clear, but it is not energetically significant. The local Me_3M^+ conformation is C_{3v} for both the C and Si cations. The geometry of $SiH_3OMe_2^+$ has also been optimized by Olsson et al.[14] The Si−O distance is HF calculated to be 1.796 Å, compared to 1.799 Å in Table 3. The HF bond energy for $H_3Si^+-OMe_2$ is 70.2 kcal/mol, and 71.1 kcal/mol is the Table 2 DFT(B3LYP) result. Experimentally, the methyl cation affinity of Me_2O has been measured at 93 kcal/mol; compared to the DFT(B3LYP) calculated 92.6 kcal/mol in Table 2. Analogously, the Me_3Si-diethyl ether ΔH BDE has been reported at 44.3 kcal/mol and Table 2 calculated to be 44.0 kcal/mol (ΔE). In general, the larger the size of R_3M^+-L, the closer are the ΔE calculated and ΔH experimental binding energies.

All the $R_3MOCH_2^+$ complexes studied here adopt a planar AMOC skeletal frame, where A is either the H, C, or F atom in the parent R group. The A−M and one ligand C−H′ bond are eclipsed and all the internal angles from A to H′ are acute. This is shown for $Me_3COCH_2^+$ in **8**. The local methyl group conformation for both Me_3C^+ and Me_3Si^+ is C_{3v}. The reason for this preferred conformation is probably steric to keep the A−M bond away from the carbonyl π system. Electrostatic or σ hyperconjugative interactions between the R_3M^+ cations and OCH_2 ligands might be expected to result in some geometry dependence on the nature of M and R, but this has not been found here.

Like the R_3MNCH^+ cations, the R_3MNCMe^+ complexes have a linear RMNCC chain backbone. The R−M and ligand C−H groups generally have a staggered conformation, although for F_3CNCMe^+ the F−C and C−H bonds are about halfway between staggered and eclipsed. The $Me_3SiNCMe^+$ cation complex is shown in **9**. The CH_3^+-NCMe (ΔH) dissociation energy has been measured at 98 kcal/mol[74] compared to the 102.9 kcal/mol DFT(B3LYP) calculated ΔE value in Table 2. For H_3Si^+-NCMe and Me_3Si^+-NCMe Olsson et al.[14] report HF bond energies of 72.3 (76.0) kcal/mol and 50.6 (49.6) kcal/mol, where the numbers in parentheses are the ΔE values from Table 2. The HF Si−N distances in $R_3SiNCMe^+$ are 1.856 and 1.902 Å for R = H and R = Me, respectively, while the corresponding DFT(B3LYP) values in Table 3 are 1.841 and 1.888 Å. In general, the DFT(B3LYP) M^+-L bond lengths are shorter than the HF calculated values, probably because of the correlation potential in the former method. Correlation enhances binding and allows a closer approach of the cation center to the ligand lone pair of electrons in dative-type bonding.[50] The Si−C bond length in the $Me_3SiNCMe^+$ complex is calculated to be 1.864 Å(HF)[14] and 1.855 Å(DFT, Table 4).

Unlike the $R_3MOCH_2^+$ complex, the $R_3MOCMe_2^+$ cations adopt a trans planar RMOC<, conformation, where R and C are trans across the M−O bond. As usual, the trimethyl cations adopt the C_{3v} conformation. The Me_3COCMe_2 cation complex is shown in **10**. Experimentally, the $Me_3Si^+-OCMe_2$ ΔH binding energy has been measured at 45.0 kcal/mol[73,75], compared with the calculated DFT(B3LYP) ΔE value of 49.5 kcal/mol in Table 2.

Like the R_3MNCH^+ and R_3MNCMe^+ cation complexes, R_3MNCF^+ has a linear MNCF chain structure. The local Me_3M^+ symmetry is C_{3v} for both the carbenium and silicenium ions. As can be seen from Tables 2 and 3, just as methyl substitution on the ligand consistently increases the R_3M^+-L binding energy and decreases the M−L bond lengths, the corresponding fluorine substitution has the opposite effect of decreasing the M−L binding energy and increasing its optimized distance. These trends are fully in accord with the dative nature of the R_3M^+-L bonding, which depends on the spatial and energetic availability of the bonding oxygen or nitrogen lone pair of electrons on L. The geometric structure of Me_3CNCF^+ is shown in **11**.

The bound $R_3MOF_2^+$ cation complexes have the expected staggered conformation between the R−M and O−F bonds across the M−O bond. However, Me_3C^+ binds OF_2 through the fluorine atoms, as shown in **12** and, therefore, has the very

long C−O distance shown in Table 3. The initial geometry of **12** was positioned in the conventional M−O binding mode. McMahon et al.[76] have discussed the preferred bonding of perfluoroamine ligands to cations through the fluorine atoms. $Me_3Si^+-OF_2$, with the Si−O bonding conformation, is barely stable at a ΔE of 7.8 kcal/mol (Table 2) and a Si−O distance of 2.297 Å (Table 3). Analogous energy and C−O distance values are calculated for $F_3COF_2^+$. In general, the $R_3M^+-OF_2$ cation complexes have the smallest binding energies for a given R and M, for all L. The $R_3MOCF_2^+$ cation complexes have a cis RCOC planar skeleton structure across C−O for the H_3C^+, H_3Si^+, and F_3Si^+ cations and a trans conformation for the Me_3C^+, $MeSi^+$, and CF_3^+. cations. The $H_3COCF_2^+$ complex is shown in **13**. The $Me_3COCF_2^+$ complex has a long C−O bond length (Table 3) and small binding energy (Table 2), although it maintains the general $R_3M^+-OCF_2$ geometric structure.

The $R_3MNF_3^+$ cation complexes have the staggered conformation. Like the corresponding OF_2 complexes, the optimized M−L bond lengths are longer than usual, except for the $CH_3^+-NF_3$ complex[14] which also has a calculated ΔE BDE of 62.0 kcal/mol. The reported experimental ΔH value is 53.6 kcal/mol[76]. The $H_3CNF_3^+$ complex is shown in **14**.

The R_3ML^+ cation complexes have been described here relative to the $R_3M^+ + L$ dissociation limit and a R_3M^+-ligand charge distribution. There are, in fact, other possible dissociation limits that would suggest other charge distributions in the complex. For example, $CH_3OH_2^+$ can derive not only from the methyl cation affinity of water but also from the protonation of ethanol. The symmetrization of $H_3COMe_2^+$ (**6**) has already been discussed above. Similarly, $MeNCMe^+$ can be considered as $MeNC + Me^+$ or $Me^+ + NCMe$. These alternative dissociation limits, which were not explored here, can be reflected in the calculated Mulliken atomic charges, tabulated in Table 5. Thus, for the CH_3L^+ complexes the charge on the carbon atom q(C) shows a substantial change from the bare H_3C^+ cation to the complexes, which reflects a delocalization of the positive charge to the ligands. The largest difference is from H_3C^+ to $H_3CNH_3^+$ where q(C) goes from +0.224 in the bare cation to −0.156 in the complex. Generally, the difference in q(C) between bare cation and complex roughly correlates with the H_3C^+-L dissociation energy, as expected. There are, however, significant variations on this trend, related possibly to the accessibility of different dissociation channels alluded to above. q(C) on the central carbon atom in the Me_3C^+ complexes varies less than in the H_3C series. However, in both the H_3Si^+ and Me_3Si^+ series, q(Si) is large and relatively constant, and usually of opposite sign to that on the coordinating ligand atom. The same situation is found for both the F_3C^+ and F_3Si^+ series.

We now turn to a discussion of the trends in the energy and geometry results tabulated in Tables 2−4, and their implications to the subject of hyperconjugative interactions in the R−M bond in these cation systems.[3,12,14,15,42,60,62,64] Comparing ΔE BDE values for R_3M^+-L from CH_3^+ to SiH_3^+ (Table 2) for a given L, there is a clear and substantial decrease in value for all the ligands. Thus, methyl cation affinity is always greater than silyl cation affinity.[3,71] On the other hand, Me_3Si^+ affinity is consistently greater than for Me_3C^+. Therefore, substitution of the methyl group for the hydrogens changes the R_3M^+-L stability order between the carbon and silicon cations. These trends have been noted before in isolated cases, both directly in the binding energies as here, and indirectly through calculated isodesmic substitution reactions.[3,14,21,42,71,77] However, certain ambiguities remained and the generality of this effect was not clear. In addition, comparing the CF_3^+ affinity with SiF_3^+ affinity to the ligands in Table 2, the same trend found for R = CH_3 is observed also for R = F, an increase in BDE values. Thus, both the methyl and fluorine substituents (R) have the same effect of causing the BDE of R_3M^+-L to be larger for the silicenium ions than in carbenium, while for the R = hydrogen substituent the opposite trend is found.

The accepted explanation for the increase in BDE from Me_3C^+-L to Me_3Si^+-L is the stronger hyperconjugative interaction in the Me_3C^+ cation compared to Me_3Si^+. Thus, formation of the Me_3ML^+ complex interferes with the Me-M^+ hyperconjugative stabilization because it uses the M^+ orbital that is available for a $R\rightarrow M^+$ interaction in the bare Me_3M^+ cation for the $L\rightarrow M^+$ dative bond in the complex. An additional factor contributing to decreased hyperconjugation in the complex is the tendency to tetrahedral symmetry about the M atom in the Me_3ML^+ complex, which decreases the optimal interaction alignment between the appropriate Me combination orbital and the "empty" orbital on M^+. Since hyperconjugative stabilization of a cation center is significant in branched carbocations,[62] the Me_3C^+-L BDE is reduced due to the differential stabilization of the bare Me_3C^+ cation compared to the complexed system. On the other hand, the bare Me_3Si^+ cations are found to be less strongly stabilized than Me_3C^+.[3,14,22,42,66,71,77] The net result is that the BDE increases from Me_3C^+-L to Me_3Si^+-L. Since the same trend is found here for F_3Si^+ relative to F_3C^+, the differential stabilization between carbon and silicon seems also to be operative in the F_3M^+ cations[78]. For the H_3M^+ cations, however, the energy ordering is consistently BDE[H_3Si^+-L] < BDE[H_3C^+-L].

Further support for the greater hyperconjugative interaction in the R_3C^+ cation for R = CH_3 and F can be found in the optimized R−M bond lengths. Thus, the C−C bond distance (Table 4) in Me_3C^+ is shortest in the bare cation and in the very weakly bound complexes with OF_2 (**12**) and NF_3 (**14**) where the ΔE binding energies are very small (2.5−4.2 kcal/mol) and the M−L distances (Table 3) are unusually large. As the ΔE binding energy gets larger and the M−L bond length decreases, the C−C distance in Me_3C^+ also increases. The latter correlations are not exact because of steric interactions between the cation and the ligand, and possible electronic effects related to interacting electron-transfer configurations. However, the shorter the C−C distance in Me_3C^+ the stronger the Me_3-C^+ hyperconjugative interaction. The largest difference in C−C distance is between bare R_3C^+ and the NH_3 or NCMe ligand cation complexes and amounts to ∼0.07 Å.

On the other hand, for the R_3Si^+-L complexes, the difference in C−Si distance between the bare Me_3Si^+ cation and the strongest Me_3SiL^+ complex is only ∼0.02 Å. This smaller difference can be taken as an indication of a much smaller hyperconjugative effect in Me_3Si^+ compared to Me_3C^+. For bare F_3C^+ compared to F_3CL^+ complexes, the situation is similar to that found for the Me_3C^+ cation; here the difference in F−C distance between bare F_3C^+ and the strongly bound $F_3CNH_3^+$ complex, for example, is again ∼0.07 Å. However, the difference in F−Si distance between F_3Si^+ and the strongly bound F_3SiL^+ complexes is only ∼0.03 Å, again an indication of a smaller F_3-Si^+ interaction compared to F_3-C^+.

We will now analyze these trends in BDE and their relationship to hyperconjugation, resonance and delocalization using the VBSCF calculations on the $AH_nMH_2^+$ model systems. The progressive increase in ΔE binding energies in Table 7 for $AH_n-MH_2^+$ as a function of VB configuration set (I−V) gives the incremental energy contribution of the configurations being

added in each step. The limiting value of the BDE was estimated in several ways; both by doing a standard G2 calculation[79] on the parent $AH_nMH_2^+$ model species and its dissociation products (AH_n and MH_2^+), and by carrying out DFT(B3LYP)/6-311+G-(2d,p) geometry optimizations with the equivalent bond constraints on the same systems. The G2 method allows no geometry constraints, so that it could not be applied to CH_3-CH_2^+ and $SiH_3CH_2^+$ which spontaneously isomerize to a different structure, as described above. The DFT(B3LYP) and G2 ΔE binding energies agree closely for $CH_3-SiH_2^+$ and $F-CH_2^+$ but differ by ~9 kcal/mol for $F-SiH_2^+$, with G2 larger; possibly because of the absence of bond equivalencies in the latter method. The CAS(4,4) BDE values are generally within ~15 kcal/mol of the DFT(B3LYP) values and are even ~1 kcal/mol larger for $CH_3-SiH_2^+$. This latter result probably just reflects an imbalance in theory level description between the complex and its dissociation products.

VBSCF(I) consists only of the simple Lewis covalent σ bond description $(AH_n):(MH_2^+)$. It provides ~50−65% of the binding for the model systems, except for $F-CH_2^+$ and $F-SiH_2^+$ which are almost unbound at this VB level. The VBSCF(I) energy minimum F−C and F−Si bond lengths (Table 8) are considerably larger than the CAS(4,4) values. Adding the $(AH_n^+)(MH_2)$ configuration (2) to give the VBSCF(II) level improves the calculated Si−C binding energies by ~43 kcal/mol for $SiH_3-CH_2^+$ and by 2 to 16 kcal/mol for the other model systems. Thus, as expected, $SiH_3 \rightarrow CH_2^+$ charge transfer (CT) to give the $(SiH_3^+)(CH_2)$ charge distribution in the σ space is a particularly important contribution to the description of the Si−C bond. Configuration 3, which represents the reverse direction CT, $AH_n \rightarrow MH_2^+$ to give the ionic $(AH_n^-)(MH_2^{2+})$ charge distribution in the σ bond space, is included in VBSCF(III). There is hardly any improvement in BDE going from VBSCF-(II) to VBSCF(III) for $CH_3-CH_2^+$ and $SiH_3-CH_2^+$, a respectable 10 kcal/mol contribution for $CH_3-SiH_3^+$, and very large ~54 and ~83 kcal/mol increases for $F-CH_2^+$ and $F-SiH_2^+$, respectively. Thus, the $(F^-)(SiH_2^{2+})$ configuration is the largest contribution to the σ bond description in $F-SiH_2^+$(80). These differences are reflected in the improved F−C, and especially F−Si, bond length values in Table 8. The VB structure weights for configuration 3 at the all-inclusive VBSCF(V) level calculation in Table 9 also show the relative importance of the a^-m^{2+} charge distribution for $FSiH_2^+$ and FCH_2^+.

The importance of the hyperconjugative interaction involving the π_a and π_m fragment orbitals, (configurations (4) to (8)), can be gauged by comparing VBSCF(IV) to VBSCF(II), or VBSCF-(III) to VBSCF(V). VBSCF(IV) adds configurations (4) to (6) to VBSCF(II). Since neither of these VB levels include configuration (3), the II → IV comparison is probably less useful for the $CH_3SiH_2^+$ and fluorine model systems where VB configuration (3) is important. For the other model systems, going from set II to set IV increases the BDE for $CH_3-CH_2^+$ by ~21 kcal/mol, while for $SiH_3-CH_2^+$ the improvement is only ~3 kcal/mol. Comparing VBSCF(V) to VBSCF(III) give similar resonance stabilizations of ~19 kcal/mol and ~4 kcal/mol for these same respective systems. VBSCF(V) includes all eight VB configurations, while VBSCF(III) has only (1) to (3). Going from set III to set V increases the BDE of $CH_3-SiH_2^+$ by ~6 kcal/mol, $F-CH_2^+$ by ~48 kcal/mol, and $F-SiH_2^+$ by ~23 kcal/mol. Thus, in $CH_3-CH_2^+$ and $CH_3-SiH_2^+$, which are model systems for Me_3C^+ and Me_3Si^+, respectively, the $\pi_a-\pi_m$ interaction contributes ~20 kcal/mol and ~6 kcal/mol, respectively, to the $CH_3-MH_2^+$ binding energies. For the corresponding $F-CH_2^+$ and $F-SiH_2^+$ species, which are model systems for F_3C^+ and F_3Si^+, the $\pi_a-\pi_m$ interaction contributes about twice the energy lowering to the BDE of $F-CH_2^+$ than to $F-SiH_2^+$. These ratios are about the same as those found by previous investigators between carbenium and silicenium systems on the basis of dissociation energies and isodesmic reactions,[3,14,21,42,71,77] and in this study of the cation complexes based on trends in R_3M^+-L binding energies and C−C and C−Si bond length changes in going from the bare R_3M^+ cations to the ligand complexes. Consistent with these results, it has also been noted by Xie et al.[24] that although hyperconjugative stabilization may be larger in carbenium ions than in silicenium ions the effect in the latter is not negligible. The results here, both in the cation/complexes comparisons and in the VB analysis, show that fluorosilicenium ions show especially significant F−Si π interactions.

The $AH_n-MH_2^+$ binding energies calculated at the VBSCF-(VI) level are seen to be the largest of all the configuration sets. Delocalization mixing between the AH_3 and MH_2^+ fragments is an effective means of introducing both charge transfer and π bonding configurations. These individual contributions are, however, not separable into their individual fragment localized contributions, as is done in sets I to V. More localized fragment configurations than were used in VBSCF-(V) are needed to reach the VBSCF(VI) theory level.

4. Summary

R_3M^+-L bond dissociation energies and R−M, M−L bond lengths in the bare cation (R_3M^+) and cation−ligand complexes have been calculated using density functional theory for a large set of such systems (M = C and Si; R = H, CH_3 and F; L = NH_3, H_2O, HCN, H_2CO, MeCN, Me_2O, Me_2CO, FCN, F_2O, F_2CO, and NF_3). For all ligand substrates, the cation−L bond energies are predicted to decrease from carbenium to silicenium with R = H but increase for R = CH_3 and F. These trends are in contrast to that found for the neutral R_3M-X homolytic bond dissociation energies (to give $R_3M^\cdot + X^\cdot$ radicals), which increase from M = C to M = Si for X substituents that bind to R_3M through an electronegative element (N, O, halogen).

For the cation−ligand systems with R = CH_3 and F, the R−M distance increases in going from the bare cation to the complexes, and increases more than twice as much for M = carbon than for M = silicon.

These results indicate that a hyperconjugative R−M interaction is operative in the bare carbenium cations with R = CH_3 and F to a much larger extent than for R = H, for any R_3Si^+, or for all the cation−ligand complexes studied here, irrespective of R.

The nature of the hyperconjugative interaction is probed using ab initio VB theory on model $AH_n-MH_2^+$ systems (AH_n = CH_3, SiH_3, and F). The results show a significant π component to the R−M bond which manifests itself preferentially both in the R−M bond energies and bond distances both for $CH_3-CH_2^+$ relative to $CH_3-SiH_2^+$ and $F-CH_2^+$ compared with $F-SiH_2^+$. However, in $F-SiH_2$ this π interaction or delocalization is still significant. The π donor ability of fluorine in group IV cations and neutral molecules has recently been discussed.[23b,78,81]

Acknowledgment. We thank Dr. Pinchas Aped for producing the figures. This work was supported by a grant from the Israel Science Foundation (Grant 484/95).

References and Notes

(1) Kutzelnigg, W. *Angew. Chem., Int. Ed. Engl.* **1984**, *23*, 272.
(2) Pauling, L. *The Nature of the Chemical Bond*, 3rd ed.; Cornell University Press: Ithaca, NY, 1960. Pauling, L. *Proc. R. Soc. London, Ser. A* **1977**, *356*, 433.

(3) Apeloig, Y. In *The Chemistry of Organic Silicon Compounds*; Patai, S., Rappaport, Z., Eds.; J. Wiley & Sons: Chichester, England, 1989.
(4) Walsh, R. In *The Chemistry of Organic Silicon Compounds*; Patai, S., Rappaport, Z., Eds.; J. Wiley & Sons: Chichester, England, 1989.
(5) Leroy, G.; Temsamani, D. R.; Wilante, C. *J. Mol. Struct*. **1994**, *306*, 21.
(6) Jasinski, J. M.; Becerra, R.; Walsh, R. *Chem. Rev*. **1995**, *95*, 1203.
(7) Basch, H.; Hoz, T. In *The Chemistry of Organic Germanium, Tin and Lead Compounds*; Patai, S., Ed.; J. Wiley & Sons: Chichester, England, 1995. Basch, H. *Inorg. Chim. Acta* **1996**, *252*, 265. Basch, H.; Hoz, Z. Unpublished results.
(8) Basch, H. *Inorg. Chim. Acta* **1996**, *242*, 191.
(9) Lambert, J. B.; Kania, L.; Zhang, S. *Chem. Rev.* **1995**, *95*, 1191. Xie, Z.; Manning, J.; Reed, R. W.; Mathur, R.; Boyd, P. D. W.; Benesi, A.; Reed, C. A. *J. Am. Chem. Soc.* **1996**, *118*, 2922.
(10) Olah, G. A.; Li, X.-Y.; Rasul, G.; Prakash, G. K. *J. Am. Chem. Soc.* **1995**, *117*, 8962.
(11) Lickiss, P. D. *J. Chem. Soc., Dalton Trans*. 1333 1992.
(12) Schleyer, P. v. R.; Muller, T.; Apeloig, Y.; Siehl, H.-U. *Angew. Chem., Int. Ed. Engl*. **1993**, *32*, 1471. Reed, C. A.; Xie, Z.; Bau, R.; Benesi, A. *Science* **1993**, *262*, 402.
(13) Olsson, L.; Cremer, D. *Chem. Phys. Lett*. **1993**, *215*, 433.
(14) Olsson, L.; Ottoson, C.-H.; Cremer, D. *J. Am. Chem. Soc*. **1995**, *117*, 7460.
(15) Arshadi, M.; Johnels, D.; Edlund, U.; Ottosson, C.-H.; Cremer, D. *J. Am. Chem. Soc*. **1996**, *118*, 5120.
(16) Sekiguchi, A.; Tsukamoto, M.; Ichinohe, M. *Science* **1997**, *275*, 60.
(17) Schleyer, P. v. R. *Science* **1997**, *275*, 39. Ottosson, C.-H.; Szabo, K. J.; Cremer, D. *Organometallics* **1997**, *16*, 2377.
(18) Lauvergnat, D.; Hiberty, P. C.; Danovich, D.; Shaik, S. *J. Phys. Chem*. **1996**, *100*, 5715.
(19) Olah, G. A. *Angew. Chem., Int. Ed. Engl*. **1995**, *34*, 1393.
(20) Stone, J. M.; Stone, J. A. *Int. J. Mass Spectrom. Ion Processes* **1991**, *109*, 247. Chen, Q.-F.; Stone, J. A. *Int. J. Mass Spectrom. Ion Processes* **1997**, *165*/*166*, 195. J. A. Stone, *Mass Spectrom. Rev.* **1997**, *16*, 25.
(21) Shin, S. K.; Beauchamp, J. L. *J. Am. Chem. Soc*. **1989**, *111*, 900.
(22) Schwarz, H. In The Chemistry of Organic Silicon Compounds; Patai, S., Rappaport, Z., Eds.; J. Wiley & Sons: Chichester, England, 1989.
(23) (a) Mayr, H.; Basso, N.; Hugen, G. *J. Am. Chem. Soc*. **1992**, *114*, 3060. (b) Frenking, G.; Fau, S.; Marchand, C. M.; Grutzmacher, H. *J. Am. Chem. Soc*. **1997**, *119*, 6648. (c) Renko, M.; Liedl, K. R.; Rode, B. M. *J. Phys. Chem. A* **1998**, *102*, 771.
(24) Xie, Z.; Bau, R.; Benesi, A.; Reed, C. A. *Organometallics* **1995**, *14*, 3933.
(25) Ziegler, T. *Chem. Rev*. **1991**, *91*, 651.
(26) Handy, N. C.; Tozer, D. J.; Laming, G. J.; Murray, C. W.; Amos, R. D. *Isr. J. Chem*. **1993**, *33*, 331.
(27) J. M. Seminario P. Politzer, Eds., Modern Density Functional Theory. A Tool for Chemistry; Elsevier: New York, 1995.
(28) Kohn, W.; Becke, A. D.; Parr, R. G. *J. Phys. Chem*. **1996**, *100*, 12974.
(29) Johnson, B. G.; Gill, P. M.; Pople, J. A. *J. Chem. Phys*. **1993**, *98*, 5612.
(30) Becke, A. D. *J. Chem. Phys.* 98 **1993**, *1372*, 5648. Lee, C.; Yang, W.; Parr, R. G. *Phys. Rev. B* **1988**, *37*, 785.
(31) Baker, J.; Muir, M.; Andzelm, J. *J. Chem. Phys.* **1995**, *102*, 2063. Scheiner, A. C.; Baker, J.; Andzelm, J. *J. Comput. Chem*. **1997**, *18*, 775.
(32) Bauschlicher, C. W., Jr.; Partridge, H. J. *J. Chem. Phys*. **1995**, *103*, 1788.
(33) Basch, H.; Hoz, S. *J. Phys. Chem.* **1997**, *101*, 4416.
(34) Basch, H.; Hoz, S. *Chem. Phys. Lett*. **1998**, *294*, 117.
(35) Cooper, D. L.; Gerratt, J.; Raimondi, M. *Adv. Chem. Phys*. **1987**, *68*, 319. *Chem. Rev*. **1991**, *91*, 929.
(36) Hiberty, P. C.; Byrman, C. P. *J. Am. Chem. Soc*. **1995**, *117*, 9875.
(37) Shaik, S.; Maitre, P.; Sini, G.; Hiberty, P. C. *J. Am. Chem. Soc*. **1992**, *114*, 7861.
(38) Hiberty, P. C.; Humbel, S.; Byrman, C. P.; van Lenthe, J. H. *J. Chem. Phys*. **1994**, *101*, 5969. Hiberty, P. C.; Flament, J. P.; Noizet, E. *Chem. Phys. Lett*. **1992**, *189*, 259.
(39) Flegg, R. H.; Harcourt, R. D. *J. Mol. Struct.* **1988**, *164*, 67.
(40) Basch, H.; Aped, P.; Hoz, S. *Mol. Phys*. **1996**, *89*, 331.
(41) Pross, A. *Theoretical and Physical Principles of Organic Reactivity*; J. Wiley & Sons: New York, 1995.
(42) Basso, N.; Gors, S.; Popowski, E.; Mayr, H. *J. Am. Chem. Soc*. **1993**, *115*, 6025.
(43) Stephens, P. J.; Devlin, F. J.; Chabalowski, C. F.; Frisch, M. J. *J. Phys. Chem*. **1994**, *98*, 11623.
(44) Frisch, M. J.; Trucks, G. W.; Schlegel, H. B.; Gill, P. M. W.; Johnson, B. G.; Robb, M. A.; Cheeseman, J. R.; Keith, T. A.; Petersson, G. A.; Montgomery, J. A.; Raghavachari, K.; Al-Laham, M. A.; Zakrzewski, V. G.; Ortiz, J. V.; Foresman, J. B.; Cioslowski, J.; Stefanov, B. B.; Nanayakkara, A.; Challacombe, M.; Peng, C. Y.; Ayala, P. Y.; Chen, W.; Wong, M. W.; Andres, J. L.; Replogle, E. S.; Gomperts, R.; Martin, R. L.; Fox, D. J.; Binkley, J. S.; Defrees, D. J.; Baker, J.; Stewart, J. P.; Head-Gordon, M.; Gonzalez, C.; Pople, J. A. Gaussian 94 (Revision C); Gaussian, Inc.: Pittsburgh, PA, 1995.
(45) See, for example, Boys, S. F.; Bernardi, F. *Mol. Phys*. **1970**, *19*, 553.
(46) van Lenthe, J. H.; Balint-Kurti, G. G. *Chem. Phys. Lett*. **1980**, *76*, 138.
(47) van Lenthe, J. H.; Balint-Kurti, G. G. *J. Chem. Phys.* **1983**, *78*, 5699.
(48) Verbeek, J.; Langenberg, J. H.; Byrman, C. P.; van Lenthe, J. H. *TURTLE—An ab Initio VB/VBSCF/VBCI Program*; Utrecht University: Utrecht, The Netherlands, 1994.
(49) Klopper, W.; Kutzelnigg, W. *J. Phys. Chem*. **1990**, *94*, 5625.
(50) Basch, H.; Hoz, T. In *The Nature of the Triple Bond*; Patai, S., Ed.; J. Wiley & Sons: Chichester, England, 1994.
(51) Dunning, T. H., Jr. *J. Chem. Phys*. **1970**, *53*, 2823.
(52) S. Huzinaga, *J. Chem. Phys*. **1965**, *42*, 1293.
(53) Roos, B. O. *Adv. Chem. Phys*. **1987**, *69*, 399.
(54) Verbeek, J. Nonorthogonal orbitals in ab initio many-electron wave functions, Ph.D. Thesis, Utrecht, The Netherlands, 1990.
(55) Basch, H.; Wolk, J. L.; Hoz, S. *J. Phys. Chem.* **1997**, *101*, 4996.
(56) Stevens, W. J.; Basch, H.; Krauss, M. *J. Chem. Phys*. **1984**, *81*, 6026.
(57) Bobrowicz, F. W.; Goddard, W. A.; III, In Methods of Electronic Structure Theory; Schaeffer, H. F., III, Ed.l Plenum Press: New York, 1977; Vol. 3.
(58) Cooper, D. L.; Gerratt, J.; Raimondi, M. *Adv. Chem. Phys*. **1987**, *68*, 319.
(59) Chirgwin, B. H.; Coulson, C. A. *Proc. R. Soc. London, Ser. A* **1950**, *201*, 196.
(60) Sieber, S.; Buzek, P.; Schleyer, P. v. R.; Koch, W.; Carneiro, J. W. de M. *J. Am. Chem. Soc*. **1993**, *115*, 259.
(61) Yannoni, C. S.; Kendrick, R. D.; Myhre, P. C.; Bebout, D. C.; Peterson, B. L. *J. Am. Chem. Soc*. **1989**, *111*, 6440.
(62) Koch, W.; Liu, B.; Schleyer, P. v. R. *J. Am. Chem. Soc.* 111, 3479 1989. Schleyer, P. v. R.; Carneiro, J. W. de M.; Koch, W.; Raghavachari, K. *J. Am. Chem. Soc.* 111, 5475. Schleyer, P. v. R.; Carneiro, J. W. de M.; Koch, W.; Forsyth, D. *J. Am. Chem. Soc*. **1991**, *113*, 3990. Carneiro, J. W. de; Schleyer, P v. R. *J. Am. Chem. Soc*. **1990**, *112*, 4064.
(63) Olah, G. A.; Rasul, G.; Heiliger, L.; Bausch, J.; Prakash, G. K. S. *J. Am. Chem. Soc*. **1992**, *114*, 7737.
(64) Olsson, L.; Cremer, D. *Chem. Phys. Lett*. **1993**, *215*, 433.
(65) Hehre, W. J.; Radom, L.; Schleyer, P. v.; Pople, J. A. *Ab Initio* Molecular Orbital Theory; J. Wiley & Sons: Chichester, 1986. Snyder, L. C.; Basch, H. *J. Am. Chem. Soc*. **1969**, *91*, 2189.
(66) Lampert, J. B.; Zhang, S.; Ciro, S. M. *Organometallics* **1994**, *13*, 2430.
(67) Meot-Ner(Mautner), M.; Karpas, Z.; Deakyne, C. A. *J. Am. Chem Soc*. **1986**, *108*, 3913.
(68) Meot-Ner (Mautner), M.; Sieck, L. W. *J. Phys. Chem*. **1990**, *94*, 7730.
(69) Lias, S. G.; Bartmess, J. E.; Liebman, J. F.; Holmes, J. L.; Levin, R. D.; Mallard, W. G. *J. Phys. Chem. Ref. Data, Suppl*. **1988**, *17* (1).
(70) Li, X.; Stone, J. A. *Int. J. Mass Spectrosc. Ion Processes* **1990**, *101*, 149.
(71) Henderwork, M. L.; Frey, R.; Dixon, D. A. *J. Phys. Chem.* **1983**, *87*, 2026.
(72) Stone, J. A.; Wojtyniak, A. C. M.; Wytenberg, W. *Can. J. Chem*. **1986**, *64*, 575.
(73) (a) Wijtyniak, A. C. M.; Stone, J. A. *Int. J. Mass Spectrosc. Ion Processses* **1986**, *74*, 59. (b) Wijtyniak, A. C. M.; Stone, J. A. *Can. J. Chem*. **1987**, *65*, 2849.
(74) Deakyne, C. A.; Meot-Ner (Mautner), M. *J. Phys. Chem*. **1990**, *94*, 232.
(75) Philips, L. F. *J. Phys. Chem.* **1990**, *94*, 5265.
(76) McMahon, T. B.; Heinis, T.; Nicol, G.; Hovey, J. K.; Kebarle, P. *J. Am. Chem. Soc*. **1988**, *110*, 7591.
(77) Houle, F. A.; Beauchamp, J. L. *J. Am. Chem. Soc.* **1979**, *101*, 4067.
(78) Wiberg, K. B.; Rablen, P. R. *J. Am. Chem. Soc*. **1993**, *115*, 614.
(79) Curtiss, L. A.; Raghvachari, K.; Trucks, G. W.; Pople, J. A. *J. Chem. Phys.* **1991**, *94*, 7221.
(80) Cleveland, T.; Landis, C. T. *J. Am. Chem. Soc.* **1996**, *118*, 6020.
(81) Schlegel, H. B.; Sosa, C. *J. Phys. Chem.* **1985**, *89*, 537.